This is a repository copy of *Error analysis of the thermal cell for soil thermal conductivity measurement*.

White Rose Research Online URL for this paper:
http://eprints.whiterose.ac.uk/112201/

Version: Accepted Version

Error analysis of the thermal cell for soil thermal conductivity measurement

J. E. Low MEng PhD, Max Fordham (formerly University of Southampton)

F. A. Loveridge* BA MSc PhD, CEng, MICE, FGS, CGeol, Royal Academy of Engineering Research Fellow, University of Leeds (formerly University of Southampton)

W. Powrie FREng MA PhD, CEng, FICE, Dean Faculty of Engineering and the Environment & Professor of Geotechnical Engineering, University of Southampton

* corresponding author – F.A.Loveridge@leeds.ac.uk; University of Leeds, Woodhouse Lane, Leeds, UK

Date of revision: 4th July 2016

Number of words in main text: 4628

4 Tables and 14 Figures

Abstract

Soil thermal conductivity is an important factor in the design of energy foundations and other ground heat exchanger systems. Laboratory tests in a thermal cell are often used to determine the thermal conductivity of soil specimens. Two interpretation methods have been suggested. Analysis can be based on the assumption of one-directional heat flow and the thermal conductivity calculated using Fourier's Law. Alternatively the lumped capacitance method can be employed, using results generated as a specimen cools. In this study, six samples of London Clay were tested using a thermal cell. A finite element model of the tests was then used to determine the validity of the assumptions made in analysis. The model showed substantial heat loss through the sides of the specimens, which would impact significantly on the calculated thermal conductivity. The conditions required for the lumped capacitance method to be valid were also found not to be met. Consequently neither analysis method is recommended. A better approach would be to pursue apparatus with fewer heat losses or transient testing techniques.

Notation

A   area (m^2)

Bi   Biot number (dimensionless)

c_p specific heat capacity (J/kgK)

h   heat transfer coefficient (W/m^2K)

L   length (m)

m   mass (kg)

Q   heat flux (W)

$\dot{Q}$ heat flux per unit volume (W/m^3)

T   temperature (degrees)

t   time (s)

λ thermal conductivity (W/mK)

ρ density (kg/m^3)

Keywords

thermal conductivity, soil, thermal cell, ground source heat pumps

Error analysis of the thermal cell for soil thermal conductivity measurement

1   Introduction

Ground source heat pump (GSHP) systems provide a viable alternative to conventional heating and cooling systems in the move towards more sustainable building solutions (Banks, 2008). Heat is transferred between the ground and the building by means of a heat transfer fluid, which is pumped through a series of pipes buried in the ground. To minimise initial construction costs, the pipes may be cast into the foundations, thereby eliminating the need to make further excavations. These systems are known as energy or thermal foundations. To design such a system, it is important to model accurately the heat transfer process between the foundations and the soil. An important input parameter for such analysis is the soil thermal conductivity.

There are several different laboratory methods for measuring soil thermal conductivity e.g. Mitchell & Kao (1978), Farouki (1986). All of them fall into one of two categories, based on analysis of steady-state or transient data. At the laboratory scale, steady-state methods involve applying one-directional heat flow to a specimen and measuring the power input and temperature difference across it when a steady state is reached. The thermal conductivity is then calculated directly using Fourier's Law. Transient methods involve applying heat to the specimen and monitoring temperature changes over time. The transient data are used to determine the thermal conductivity, usually by application of an analytical solution to the heat diffusion equation. Some transient methods can also be used to assess other thermal properties such as thermal diffusivity (Bristow et al, 1994).

A steady-state method that has shown promise is the thermal cell method (Clarke et al, 2008). The main advantage of this method is that it requires minimal preparation for testing U100 (undisturbed, 100 mm diameter) samples of soil taken from routine site investigations. In this paper, the theory and experimental method are described and the limitations discussed. One particular area of concern is heat loss through the apparatus. This is investigated by modelling the thermal cell using finite element analysis, and comparing the results with models of an ideal heat lossless thermal cell.

2   Theory

The thermal cell used in this research (Figure 1a, Table 1) is based on a design and specification by Clarke et al (2008) (Figure 1b). Although other arrangements of thermal cell are used in research, e.g. Alrtimi et al (2013), the Clarke et al (2008) specification is recommended for laboratory soil thermal conductivity testing by the Ground Source Heat Pump Association (GSHPA, 2012) and remains in use in practice. In the Clarke et al (2008) method, the thermal conductivity of a 100 mm diameter 100mm high specimen is measured by generating one-directional heat flow along the axis. In both cases the heat source is a cartridge heater embedded in the lower aluminium platen. Provided that the specimen is well insulated

34 so that heat losses through the insulation and acrylic base can be neglected, steady heat flow through the
35 specimen is governed by Fourier's Law:

36 $$Q = -\lambda A \frac{\Delta T}{L}$$ **Equation 1**

37 where Q is the power input, A is the cross-sectional area, ΔT is the temperature difference across the
38 length of the specimen, and L is the length of the specimen. In applying Equation 1, the power input Q
39 must be known. If Q cannot be measured directly, measurements of the temperatures in the specimen as
40 it cools after the power is switched off (the recovery phase) can be used to determine the heat transfer
41 coefficient between the top of the soil and the air, and hence the power. This approach, proposed by
42 Clarke et al (2008), uses the lumped capacitance method, which assumes that the temperature difference
43 across the length of the soil specimen is small compared to the temperature difference between the soil
44 and the ambient air. The lumped capacitance method should only be used when the Biot number, Bi,
45 (Equation 2) is small (Incropera et al, 2007):

46 $$\frac{T_{base} - T_{top}}{T_{top} - T_{amb}} = Bi < 0.1$$ **Equation 2**

47 where subscripts `base', `top' and `amb' refer to the temperature at the base of the soil, top of the soil,
48 and of the ambient air respectively. The ambient temperature is assumed to be constant. The Biot
49 number, Bi, is a dimensionless group quantifying the ratio of resistances to heat transfer by conduction
50 and convection. Where Equation 2 is satisfied, the temperature of the soil at time, t, is (Clarke et al, 2008):

51 $$T = T_{amb} + (T_0 - T_{amb}) exp\left(-\frac{hA}{mc_p}t\right)$$ **Equation 3**

52 where T_0 is the temperature of the soil at time t=0 (when Equation 2 starts to apply), h is the convective
53 heat transfer coefficient, m is the total mass of soil, and c_p is the soil specific heat capacity. The specific
54 heat capacity is estimated from the mass-weighted properties of the soil constituents:

55 $$mc_p = m_s c_{ps} + m_w c_{pw}$$ **Equation 4**

56 where subscripts `s' and `w' refer to soil particles and water respectively. Equation 3 gives a theoretical
57 decay curve which can be fitted to the experimental data by modifying h until the two curves match. At
58 steady state, conservation of energy requires that the heat flow rate across the soil is equal to the heat
59 flow rate at the top of the specimen from the soil to the air:

60 $$Q = \lambda A \frac{T_{base} - T_{top}}{L} = hA(T_{top} - T_{amb})$$ **Equation 5**

61 This is used to calculate the thermal conductivity. It is worth mentioning that this method introduces an
62 error associated with the estimation of the bulk specific heat capacity from those of the soil constituents
63 (Equation 4), whose properties may not be accurately known.

3 Laboratory tests

3.1 Method

For clarity, the thermal cell used in this research will hereafter be referred to as the UoS (University of Southampton) thermal cell, and the thermal cell from (Clarke et al 2008) as the Clarke thermal cell. Figure 1 shows how they differ. Most notably, the UoS cell has a thicker acrylic base and thicker insulation in an attempt to minimise unwanted heat losses. The UoS cell uses expanded polystyrene as the insulation as it has a low thermal conductivity and could be easily wrapped around the soil specimen.

The top platen in the Clarke cell was used to maintain a constant temperature at the top of the specimen if a constant ambient air temperature could not be maintained. This platen was removed from the UoS cell as testing was conducted in a temperature controlled room. Instead the top of the specimen was covered with a sheet of aluminium foil to prevent the soil from drying. To measure the temperature at the top of the soil, a thermistor was mounted inside the tip of a hypodermic needle and inserted 2mm into the top of the soil, at the centre of the specimen cross-section (Figure 2).

Clarke et al (2008) monitored the temperature gradient within the specimen by pushing two hypodermic needle thermistors radially into the specimen at a height of one third and two thirds of the total height. The UoS cell did not have these additional thermistors, as the soils were too hard for the hypodermic needles to be inserted. Even if this were not the case, the needles would cause additional disturbance to the soil and require holes in the insulation for insertion the needles, potentially forming thermal bridges.

Tests were carried out on six samples of London Clay taken from different depths within a ground investigation borehole at a central London development site. Prior to the thermal cell tests, the thermal conductivities of the samples were measured with a needle probe (Hukseflux Thermal Sensors2003), which is a standard transient method. The results from these tests (Low et al, 2015, Low, 2016) were used in the thermal cell numerical models (see Section 4.2.2).

Two 100 mm long specimens were cut from each sample; hereafter these are referred to as `top half' and `bottom half' for each depth. To carry out a test, the cartridge heater was turned on and the power controlled so that the platen remained at a constant temperature of 40°C. Temperatures were monitored until a steady state was reached, and maintained for a period of at least 2 hours. The power to the cartridge heater was then switched off, and the temperature during the recovery period monitored.

In contrast to the examples presented in Clarke et al (2008), in none of twelve London Clay tests were the temperatures at the top and bottom of the soil similar during recovery. Therefore, the Biot number never fell below 0.1 and the power could not be calculated using the lumped capacitance method. Instead the applied power had to be measured directly. The data logger was programmed to record when the cartridge heater switched on and off. The average power applied during the steady state stage could then be calculated from the known cartridge heater power of 50 W.

3.2   Results

99   A typical test result is shown in Figure 3. Table 2 shows the specimen properties at steady state and the
100   calculated thermal conductivity. The thermal conductivities for all the specimens are shown in Table 3 and
101   are within the expected range for London Clay (e.g. Banks et al, 2013).

102   While the experiments were fairly straightforward and the data simple to interpret, the results were
103   consistently higher than those determined using the needle probe apparatus (Low et al, 2015, Low, 2016).
104   This led to concerns about heat losses through the acrylic base and insulation, which are investigated in
105   the following section.

106   # 4   Numerical modelling

107   Potentially the greatest source of error in the thermal conductivity method is in determining the power
108   input. The interpretation of the experimental results described above does not take into account any heat
109   losses that may occur through the base and insulation. Numerical modelling using the finite element
110   software COMSOL was used to determine the significance of this effect. Three models were constructed
111   to represent: (a) the UoS cell, (b) the Clarke cell, and (c) an ideal lossless cell. The models were 2D
112   axisymmetric, and assumed no change in thermal properties of the materials with temperature. The
113   models were used to determine the heat losses, and to discover why the UoS temperature decay data did
114   not satisfy the criterion for using the lumped capacitance method, while that given in Clarke et al (2008)
115   appears to have done so.

116   ## 4.1   Modelling heat transfer

117   Heat transfer in a solid is governed by the heat diffusion equation:

118   $$\rho c_p \frac{\delta T}{\delta t} - \nabla \cdot (\lambda \nabla T) = \dot{Q}$$
   Equation 6

119   where ρ is the mass density, c_p is the heat capacity, T is temperature, t is time, λ is the thermal
120   conductivity, and $\dot{Q}$ is the heat flux per unit volume.

121   The three models were meshed using triangular elements of maximum size 2 mm. Mesh sensitivity using
122   a heat balance was carried out that showed this degree of discretisation produced >99.7% of the expected
123   result and was therefore acceptable.

124   ## 4.2   UoS thermal cell

125   The model of the UoS thermal cell is shown in Figure 4a. The following sections outline how the properties
126   of the model were chosen. Steady state and transient simulations were carried out, depending on the
127   required output. For the steady state analysis, a constant power was specified for a heat source in the
128   aluminium platen, simulating the cartridge heater. Alternatively, a constant temperature condition at the

129 top of the platen could be used. For the transient analysis, a constant heat source would be
130 unrepresentative of the actual thermal cell, because the power varies initially to maintain a constant
131 temperature of 40°C. Therefore, the heat source was replaced by a constant temperature condition at the
132 top of the platen during the heating phase, which was disabled during the recovery phase. Heat losses
133 and the suitability of the lumped capacitance method were investigated using these transient simulations.

134 *4.2.1   Material properties*

135 Unless stated otherwise, the material properties used in the models were as shown in Table 4. The
136 ambient temperature and the initial temperature of the thermal cell were the same, 20°C.

137 *4.2.2   Heat transfer coefficient*

138 The external boundary conditions were all assumed to be convective with the heat flux at the boundary
139 determined by a heat transfer coefficient, h (W/m^{2}K). The heat transfer coefficient between the top and
140 sides of the UoS thermal cell and the surrounding ambient air had to be determined. To do this, steady
141 state analyses were run for heat transfer coefficients from 10 to 35 W/m^{2}K, with the temperature at the
142 top of the platen set to 40°C. The temperature at the top of the specimen during steady state was obtained
143 from the output. This was compared with the experimentally measured top temperature for the 8.00 -
144 8.45 m depth top specimen, and the 19.00 - 19.45 m depth top specimen. The soil thermal conductivities
145 in the models were set to the values measured by the needle probe at the relevant depths, 1.32 W/mK
146 and 0.96 W/mK respectively. The average heat transfer coefficient was found to be 15 W/m^{2}K, which was
147 used in subsequent simulations.

148 During these simulations, the boundary between the thermal cell base and the laboratory bench on which
149 it stood was modelled as convective with a heat transfer coefficient of 5 W/m^{2}K. A sensitivity study was
150 carried out for this parameter, which was varied between 0 and 25 W/m^{2}K while the heat transfer
151 coefficient at the other boundaries was set at 15 W/m^{2}K as determined previously. It was found that
152 varying the base heat transfer coefficient had a negligible effect on the results, perhaps because of the
153 relatively small surface area of the thermal cell in contact with the bench. Therefore, the initial assumption
154 of 5 W/m^{2}K was maintained in subsequent simulations.

155 *4.2.3   Heat losses*

156 The main objective of the numerical simulation was to determine the significance of heat losses in the
157 thermal cell laboratory tests. This was done using the steady state analysis. In the UoS thermal cell model,
158 a constant power to the cartridge heater was specified (with the source located at the centre of the platen)
159 and adjusted until a soil base temperature of 40°C was achieved, and the heat fluxes at the top and bottom
160 of the soil at steady state were used to calculate an average heat flux through the soil. The thermal
161 conductivity of soils tends to lie in the range of 0.2 to 5 W/mK (GSHPA, 2012). For this range, the power
162 loss was calculated as:

163 $$Power\ loss\ (\%) = \frac{Q - (Q_{top} + Q_{bottom})/2}{Q} \times 100$$ **Equation 7**

164   where Q is the total power supplied to the cartridge heater, and subscripts `top' and `bottom' refer to the
165   heat flux at the top and bottom of the soil specimen respectively. Figure 5 shows that the power loss is
166   significant, particularly for soils of low thermal conductivity, with power losses of between 35% and 75%.
167   This makes it difficult to determine what value of power to use in thermal conductivity calculations for
168   the actual thermal cell. Above 3.5 W/mK it may be possible to estimate the power going through the soil
169   as 35% less than the power to the cartridge heater. Below 3.5 W/mK the power going through the soil is
170   much more dependent on the soil thermal conductivity. For any soil, estimating the power going through
171   the soil as 35% less than the power to the cartridge heater would be an improvement to the thermal
172   conductivity calculation.

173   Figure 6a shows the temperatures in the thermal cell as an isothermal contour plot. The boundary heat
174   fluxes were aggregated to determine where the heat was being lost; the results are shown in Figure 7 for
175   a soil specimen of conductivity 2.75 W/mk. This indicates that heat is lost through both the insulation and
176   the base. Although it might be possible to reduce heat loss through the insulation by using better materials
177   or a vacuum, the base must provide a stable platform to support the other components, while having as
178   low a thermal conductivity as possible. It would be difficult to find a material that performs better in these
179   respects than acrylic, so it is unlikely that base heat losses would be further reduced with a similar
180   specimen arrangement. This problem can be addressed by testing two specimens that sandwich the
181   heater as in standard guarded hot plate method (BSI, 2001). However, this apparatus requires much larger
182   specimen sizes and hence is not really suitable for soils. Nonetheless the principle can be adopted for
183   soils in bespoke apparatus, e.g. Alrtimi et al (2013).

184   One possible way of reducing the radial heat loss is to reduce the thickness of the specimen. For a range
185   of thicknesses, the power to the cartridge heater was varied until a base temperature of 40°C was reached.
186   The thermal conductivity was then calculated using the total power and temperature difference across
187   the specimen (Figure 8). Errors do reduce for thinner specimens, but even for a thickness of 10 mm, the
188   calculated thermal conductivity was significantly different from the thermal conductivity specified in
189   setting up the model. Smaller thicknesses would not be feasible from an experimental point of view.

190   In experiments by Alrtimi et al (2013), a similar method of calculating the thermal conductivity at different
191   specimen lengths was applied in practice. They extrapolated from these values to find the thermal
192   conductivity for a theoretical zero length specimen. This should reduce the influence of radial heat losses
193   on the calculated thermal conductivity, but considering the value of thermal conductivity at zero thickness
194   from Figure 8 it is suggested that this approach cannot totally compensate for radial losses and that large
195   errors may still remain.

196 *4.2.4   Time-dependent response and recovery curve*

197 The transient model was able to produce a time-dependent simulation of the UoS thermal cell for

198 comparison with the experimental results (Figure 9). During the heating phase, the power to the cartridge

199 heater was not constant but was varied to keep the temperature at the base of the soil constant.

200 Therefore, to obtain a time-dependent result reflecting to the experimental setup, the constant power

201 condition was replaced with a constant temperature boundary condition of 40°C applied at the base of

202 the soil during the heating phase. During the recovery phase this constant temperature was disabled and

203 the temperatures within the soil allowed to find their own equilibrium. All other external boundary

204 conditions remained unchanged.

205 For the thermal cell tests on the London Clay samples, the recovery curve could not be used to estimate

206 the power as the temperature difference across the soil was too large for the lumped capacitance method

207 to apply. The Biot number during recovery is plotted for both the UoS thermal cell numerical model and

208 for the laboratory test on the 8.00-8.45 m depth top specimen in Figure 10. The Biot number in the model

209 was higher than in the laboratory test, and did not gradually decrease. This is because the recovery

210 temperatures in the model decreased more rapidly than in the laboratory test, which could be due to

211 imperfect contacts at boundaries in the test, such as between the soil and the insulation, which would

212 slow the rate of temperature decrease. This effect can also be seen during the heating phase, where the

213 top temperature rises more rapidly in the model. Alternatively, it may be that the thermal conductivity

214 and heat transfer coefficient values used in the simulations do not match those in the real experiments.

215 Despite the difference in shape of the two graphs, the Biot number never fell below 0.1 in either case.

216 Therefore, the lumped capacitance method is not recommended for calculating the power in a UoS

217 thermal cell test. The power should instead be measured directly.

218 **4.3   Clarke thermal cell**

219 In Clarke et al (2008) a theoretical decay curve was fitted to the recovery data to determine the power

220 applied to the soil specimen. The temperature difference through the soil was small during recovery,

221 allowing the lumped capacitance method to be used. A model of the Clarke cell was made (Figure 4b) to

222 determine whether this could be the case, and how and why the recovery curve may differ from the UoS

223 thermal cell. The model dimensions were the same as the Clarke cell (Figure 4), except for the removal of

224 the top aluminium plate and platen. This was the configuration adopted for a test on saturated fine

225 Leighton Buzzard sand (Clarke, 2015 pers. comm.), the result of which was given in Clarke et al (2008) and

226 is used here for comparison. The material properties were assumed to be the same as in the model of the

227 UoS cell, which were given in Table 4. The ambient temperature in the laboratory was approximately 12°C,

228 less than that in the Southampton tests. This resulted in a lower specimen top temperature (30.6°C) for a

229 comparable base temperature (40.8°C) at steady state.

230 The thermal conductivity of the soil in the model was set to 2.75 W/mK, which was measured by Clarke

231 et al (2008) in their experiment using the thermal cell on a specimen of Leighton Buzzard sand. Clarke et

232 al (2008) assumed a heat transfer coefficient of 25 W/m²K and initially this value was used on all external
233 boundaries of the model. However, the shape of the resulting temperature-time graph was significantly
234 different from the experimental data reported in Clarke et al (2008). The heat transfer coefficient and the
235 thermal conductivity were individually varied until the experimental steady-state temperature of 30.6°C
236 at the top of the specimen was reached, to see if a closer fit could be achieved. This did not produce a
237 graph that was similar to the experimental result. However, when both the soil thermal conductivity and
238 the heat transfer coefficient were varied, a similar graph was achieved (Figure 11). Using this model, a
239 significant portion of the recovery curve had a Biot number just above 0.1, as in Figure 12. It could be
240 argued that based on this, it may be inappropriate to use the lumped capacitance method to determine
241 the power input. Additionally, the model fit was only achieved by using a model thermal conductivity of
242 1.4 W/mK, compared with an experimental thermal conductivity of 2.75 W/mK. The fitted value of the
243 heat transfer coefficient was 4.4 W/m²K.

244 Compared with the recovery of the UoS thermal cell results, the top and base temperatures of the Clarke
245 cell converge much more rapidly. This is possibly due to greater heat losses through the insulation and
246 base, resulting in a more rapid decrease in temperature at the specimen base. The losses at steady state
247 are shown in Figure 6b. The temperature of the acrylic base has been raised significantly by the power
248 supplied to the cartridge heater.

249 The alternative to the lumped capacitance method would be to measure the power directly for use in the
250 thermal conductivity calculation. However, the heat losses through the insulation and base in Figure 6 are
251 clearly greater than those for the UoS thermal cell. Hence direct measurement of the heater power would
252 lead to an incorrect calculation of the thermal conductivity unless losses accounted for specifically.

253 **4.4 Ideal thermal cell**

254 The lumped capacitance method was unsuitable for use with the UoS thermal cell due to the Biot number
255 never falling below 0.1 during the recovery phase of the test. Numerical simulation of the Clarke thermal
256 cell showed that the Biot number did approach 0.1 as the temperature in the soil specimen converged
257 more rapidly during recovery. However, this superficially better fit to the lumped capacitance method is
258 most likely to be caused by greater heat losses from the Clarke thermal cell compared with the UoS
259 thermal cell.

260 To explore the effect of heat losses on the recovery phase of the test further and to examine whether the
261 lumped capacitance method would ever be applicable, a further numerical model of a perfectly insulated
262 thermal cell was produced (Figure 4c). At the base was a thin disk (1 mm thickness) with the same
263 properties of the soil. This is because COMSOL could not model a boundary with a constant temperature
264 condition that was also perfectly insulating. Therefore, a constant temperature condition was defined at
265 the top of the disk, and the base was perfectly insulated. The upper surface of the specimen was retained
266 as a convective boundary condition with an assumed heat transfer coefficient of 25 W/m²K.

267   The model was run for different values of soil thermal conductivity. For each value, a theoretical curve
268   (see Equation 3) based on the lumped capacitance method was fitted to the numerical model recovery
269   curve, and then the thermal conductivity was calculated based on the theoretical curve. The results of this
270   analysis are shown in Figure 13. It can be seen that the higher the thermal conductivity, the more closely
271   the theoretical curve resembles the model curve. Hence, the thermal conductivity calculated using the
272   theoretical curve becomes closer to the model value as the thermal conductivity increases, as shown in
273   Figure 14. Calculation of the minimum Biot number for each simulation shows how this decreases as the
274   thermal conductivity increases (Figure 14). Furthermore, errors in thermal conductivity determination of
275   less than 10% are only obtained once the Biot number has fallen below a value of 0.1 which occurs at
276   approximately 13 W/mK thermal conductivity.

277   Typically, soil thermal conductivity ranges between 0.2 and 5 W/mK (GSHPA, 2012). Within this range of
278   soil thermal conductivities, the lumped capacitance method would give a significant underestimate of the
279   thermal conductivity for an ideal thermal cell, according to the numerical analysis. Interestingly, the
280   reason why the Biot number remains large is because of the lack of heat losses. The significant difference
281   in temperature between the base and top of the soil specimen is due to the heat being dissipated much
282   more rapidly from the top by convection, while the base has insulation on all sides slowing the rate of
283   temperature decrease. Comparison of the results for the UoS, Clarke and ideal thermal cells shows that
284   at realistic soil thermal conductivities increasing the heat losses improves the apparent fit of the response
285   curve to the theoretical solution, albeit with the wrong parameter values. On this basis it might be argued
286   that for a poorly insulated thermal cell, the power would be better estimated using the lumped
287   capacitance method, and for a well insulated thermal cell the power should be measured directly.
288   However, both these approaches have still be shown to lead to appreciable errors in the estimation of the
289   specimen thermal conductivity. This demonstrates the difficulty of determining the correct power, and
290   calls into question the validity of the thermal cell method.

291   **5   Conclusions**

292   Laboratory testing using a thermal cell based on the specification of Clarke et al (2008) has shown that
293   the temperature difference across the soil is too great for the lumped capacitance method to be used
294   during the recovery phase as a means of calculating the power. The power should instead be measured
295   directly, for example using the data logger to record when the cartridge heater was switched on and off.

296   Numerical modelling has shown that the UoS thermal cell has significant heat losses of at least 30% over
297   the range of typical soil thermal conductivities. This would impact the thermal conductivity calculated
298   from a laboratory test. Similarly, the numerical model showed a significant temperature difference across
299   the soil during the recovery phase of the test, confirming that the lumped capacitance method was not
300   appropriate. A second numerical model simulating the Clarke cell also showed this to be the case.

Analyses using a numerical model of an ideal (perfectly insulated) thermal cell showed that for the range of soil thermal conductivities, the lumped capacitance method would give a significant error in the calculated thermal conductivity. Only for thermal conductivities above 15 W/mK did this error fall below 10%.

This research has shown that neither the UoS nor Clarke thermal cells give accurate results because of the significant and unavoidable effects of heat losses. The heat losses vary depending on the type of soil, with the lowest thermal conductivity soils having the highest heat losses, potentially over 50%. Even for quartz rich higher thermal conductivity soils heat losses will always exceed 30% for the types of thermal cell examined. The lumped capacitance method is unlikely to be applicable for realistic soil thermal conductivities since the approach only gives an apparently good fit to the theoretical curve on a cell with significant heat losses and in such cases the parameter values are then wrong. If the power could be measured directly, eliminating the need for the lumped capacitance method, and heat losses were drastically reduced, a more accurate thermal cell could be developed. However, arrangements similar to those presented in this paper potentially lead to significant errors in thermal conductivity determination. Hence transient measurement methods are preferable if heat losses cannot be controlled sufficiently.

Acknowledgements

References

Alrtimi AA, Rouainia M and Manning DAC (2013) Thermal enhancement of PFA–based grout for geothermal heat exchangers. Applied Thermal Engineering 54: 559–564.

Banks D (2008) An introduction to thermogeology: ground source heating and cooling. Blackwell Publishing Ltd.

Banks, D., Withers, J. G., Cashmore, G., & Dimelow, C. (2013), An overview of the results of 61 in situ thermal response tests in the UK, Quarterly Journal of Engineering Geology & Hydrogeology, 46, 281-291.

Bristow KL, Kluitenberg GJ and Horton R (1994) Measurement of Soil Thermal Properties with a Dual-Probe Heat-Pulse Technique. Soil Science Society of America Journal 58: 1288–1294.

333 BSI (2001), BS EN 12667:2001 Thermal performance of building materials and products – Determination
334 of thermal resistance by means of guarded hot plate and heat flow meter methods – Products of high and
335 medium thermal resistance, BSI, London.

336 Clarke BG, Agab A and Nicholson D (2008) Model specification to determine thermal conductivity of soils.
337 Proc ICE Geotechnical Engineering 161: 161–168.

338 Farouki O (1986) Thermal properties of soils. Series on rock and soil mechanics, Trans Tech.

339 GSHPA (2012) Thermal Pile Design, Installation & Materials Standards. Ground Source Heat Pump
340 Association, Milton Keynes.

341 Hukseflux Thermal Sensors (2003) TP02 Non-Steady-State Probe for Thermal Conductivity Measurement
342 – manual v0908. Hukseflux Thermal Sensors, Delft.

343 Incropera FP, DeWitt DP, Bergman TL and Lavine AS (2007) Fundamentals of Heat and Mass Transfer. 6
344 edn., John Wiley & Sons Inc.

345 Jablite Intelligent Insulation (2014) Jablite Classic Expanded Polystyrene Technical Information.
346 http://www.jablite.co.uk/site/datasheets/6/6.pdf.

347 Low, J. E. (2016) Thermal conductivity of soils for energy foundation applications, PhD thesis, University
348 of Southampton.

349 Low, J. E., Loveridge, F. A., Powrie, W. & Nicholson, D., 2015. A comparison of laboratory and in situ
350 methods to determine soil thermal conductivity for energy foundations and other ground heat exchanger
351 applications, Acta Geotechnica 10(2), 209–218.

352 Mitchell JK and Kao TC (1978) Measurement of soil thermal resistivity. Journal of the Geotechnical
353 Engineering Division 104: 1307–1320.

354

Table 1 Dimension of UoS Thermal Cell

Material	Dimensions (cm)
Acrylic base	8.8 (maximum, at centre) x 15
Soil Specimen	10 x 10
Insulation	18 (height) x 7 (radial thickness)

Table 2 Example Results for the Thermal Cell Test

Sample Depth (m)	8.00 – 8.45
Specimen	Top half
Diameter (mm)	103
Length (mm)	106
Base temperature (^{o}C)	40.1
Top temperature (^{o}C)	28.4
Power (W)	1.85
Thermal Conductivity (W/mK)	**2.01**

Table 3 Thermal Cell Thermal Conductivity Results for all London Clay Samples

Sample Depth (m)	Thermal Conductivity (W/mK)	
	Top Half Specimen	Bottom Half Specimen
2.00–2.45	1.86	1.72
8.00–8.45	2.01	1.88
10.00–10.45	1.85	1.91
17.00–17.45	1.92	1.88
19.00–19.45	1.65	1.75
21.50–21.95	2.19	1.84

Table 4 Model Material Properties

	Soil[1]	Aluminium	Acrylic	Insulation[2]
Thermal conductivity (W/mK)	2.75	160	0.18	0.03
Specific heat capacity (J/kgK)	1632	900	1470	1130
Density (kg/m^3)	2010	2700	1190	23

1. Clarke et al, 2008; 2. Jablite Intelligent Insulation, 2014)

Figure 1 Cross section diagrams of a) the University of Southampton (UoS) thermal cell; and b) the Clarke thermal cell. In both cases the heat source is a cartridge heater embedded within the lower aluminium platen.
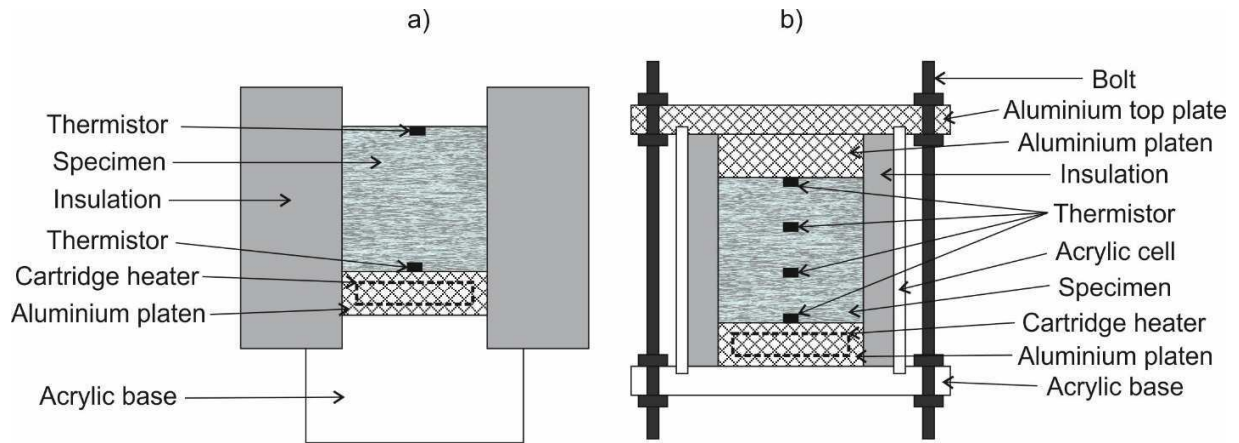
Figure 2 The UoS thermal cell showing the entire cell with insulation (left) and the base only (right)
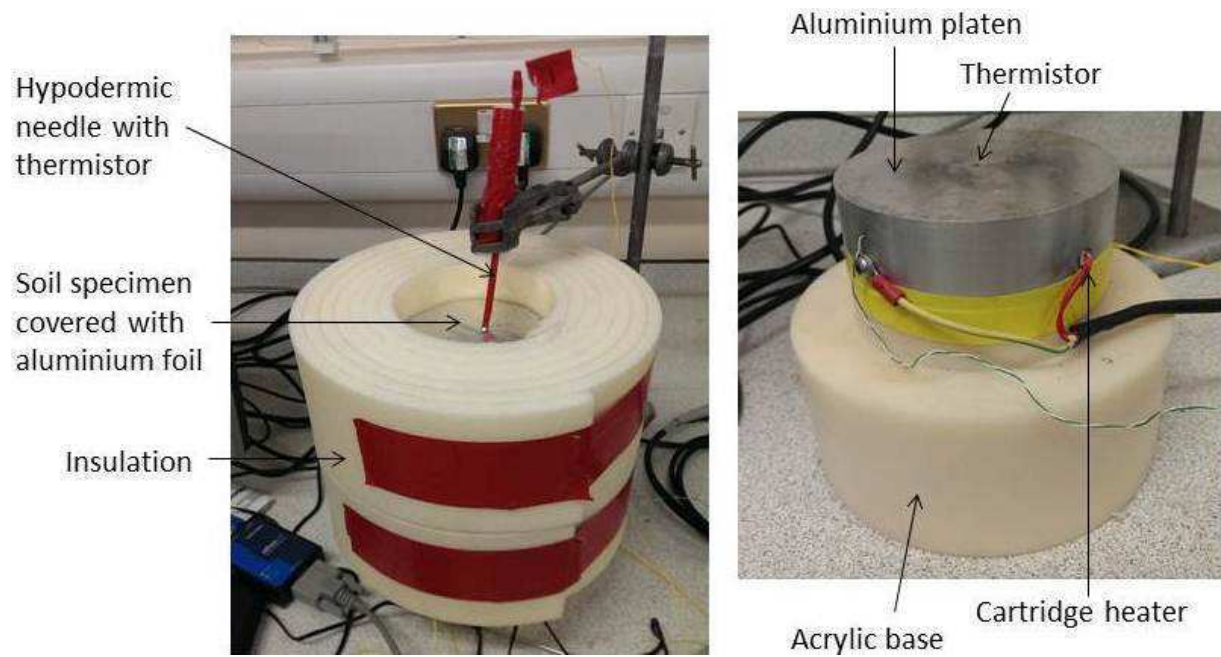
Figure 3 Thermal cell results for the top half of the 8.00 – 8.45m depth sample showing the measured temperatures and the calculated Biot number during recovery.
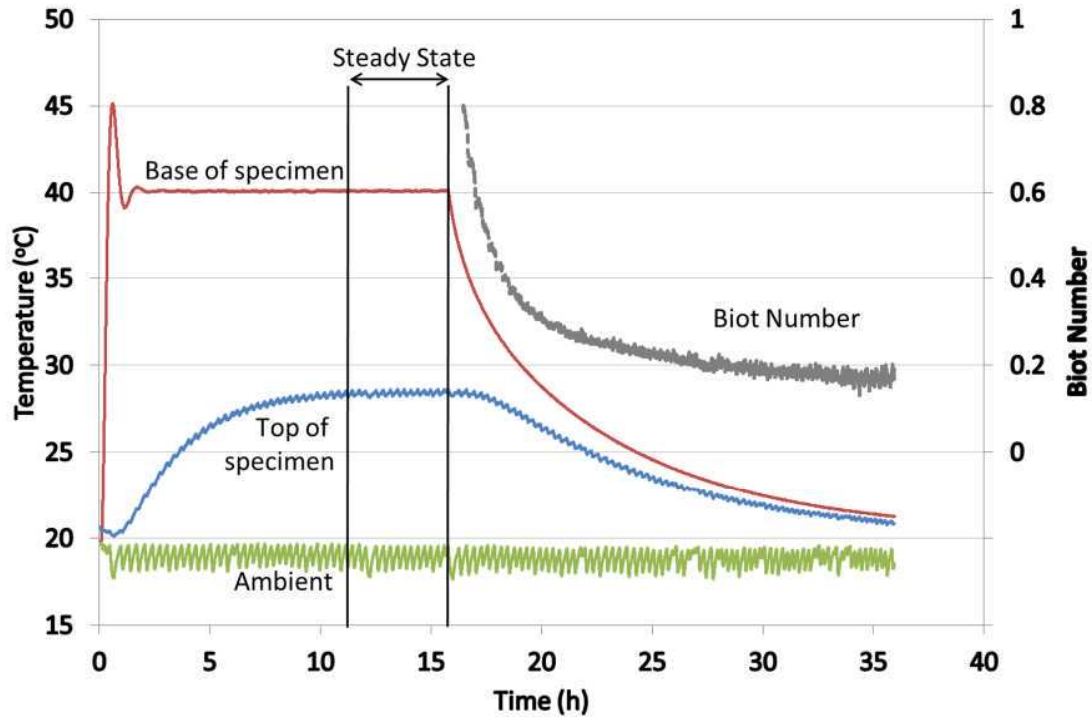

Figure 4 Model cross section showing materials and boundary conditions a) UoS thermal cell; b) Clarke thermal cell; c) idealised (perfectly insulated) cell.
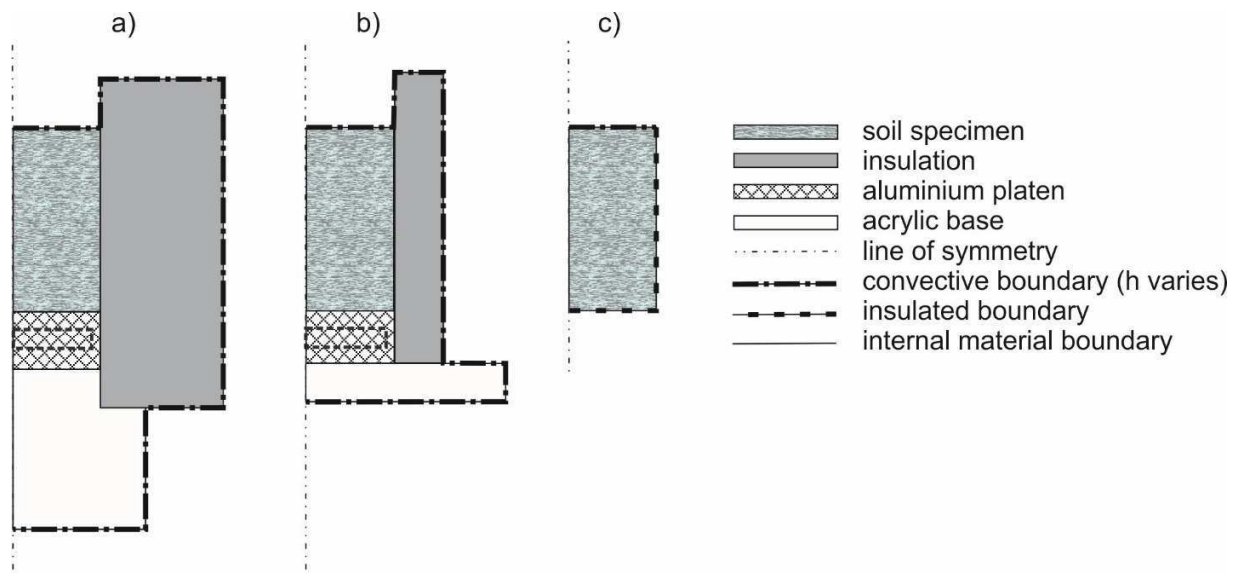
Figure 5 UoS thermal cell model: power loss for different soil thermal conductivities
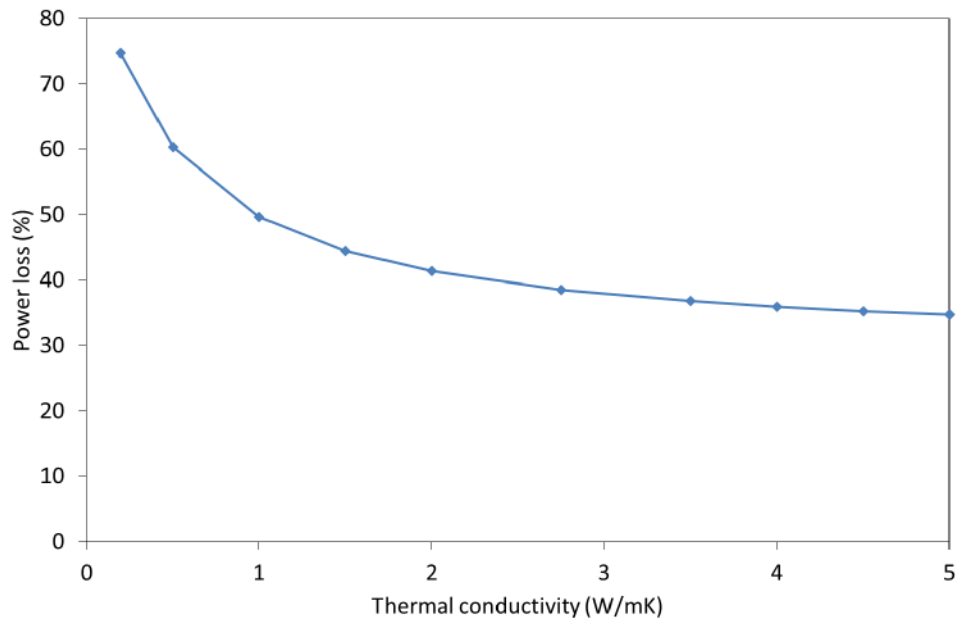
Figure 6 Numerical model results showing isothermal contours at 2°C intervals for soil thermal conductivity of 2.75 W/mK a) the UoS thermal cell; b) Clarke cell. In both cases the direction of heat flow is shown by arrows with lengths proportional to the relative heat flux magnitude.
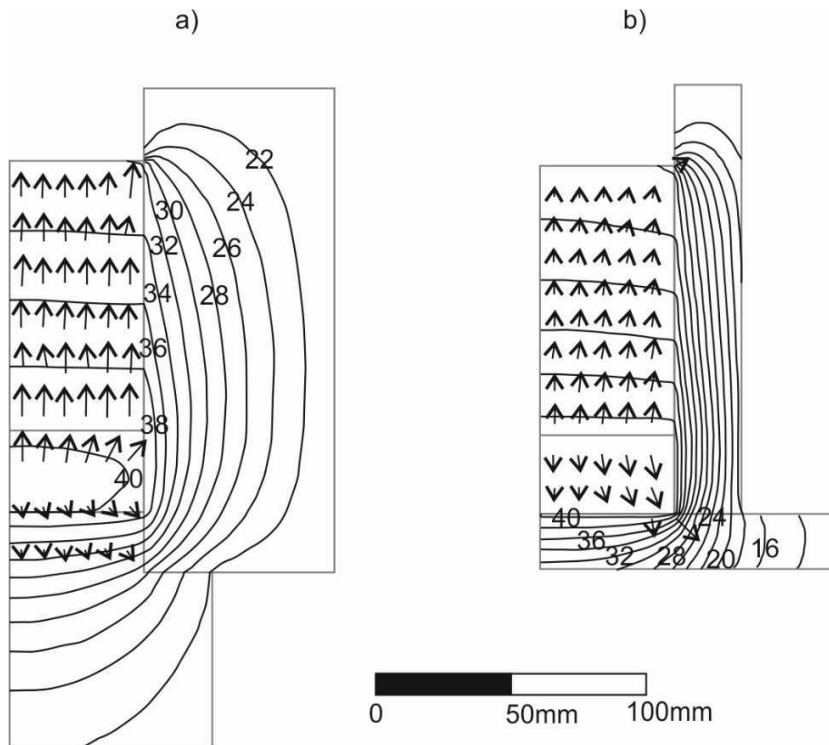
Figure 7 Heat flow balance for the modelled UoS thermal cell assuming a soil thermal conductivity of 2.75 W/mK. The total heat is supplied by the cartridge heater at A.
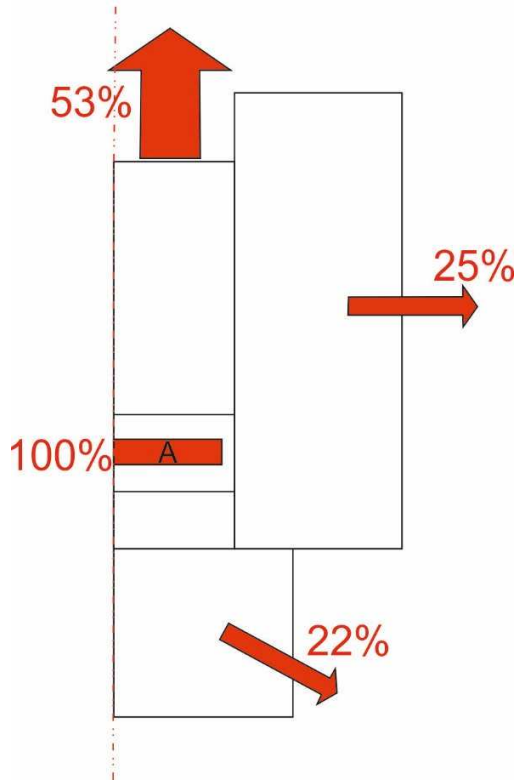
Figure 8 Calculated soil thermal conductivity for specimens of different thickness, based on the UoS thermal cell model, with a specified soil thermal conductivity of 2.75 W/mK.
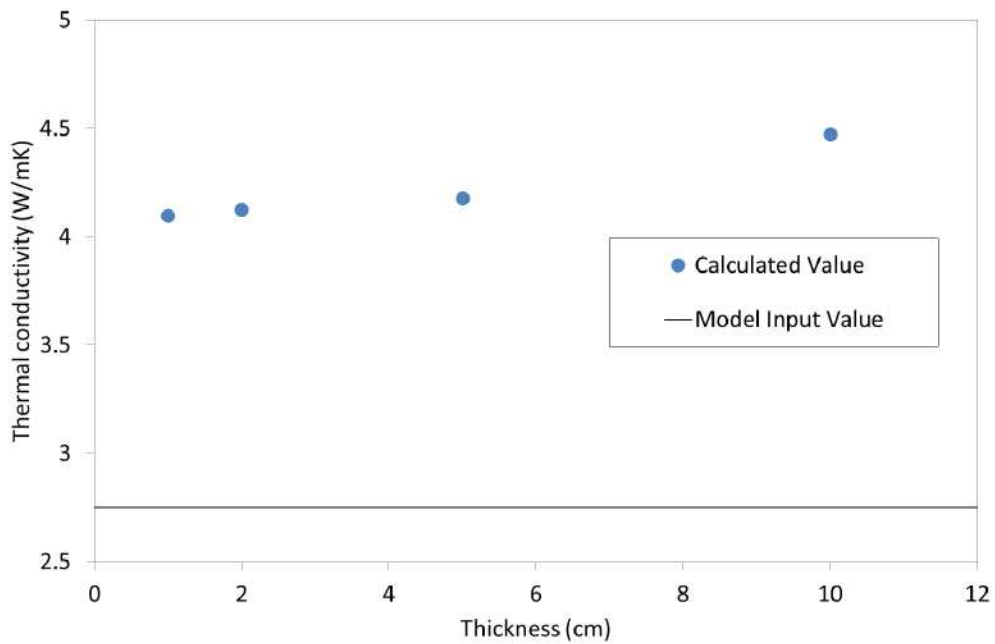
Figure 9 Comparison of the laboratory and modelled temperature variation with time for the UoS thermal cell for the 8.00 – 8.45m depth top specimen. Model assumes a soil thermal conductivity of 1.32 W/mK.
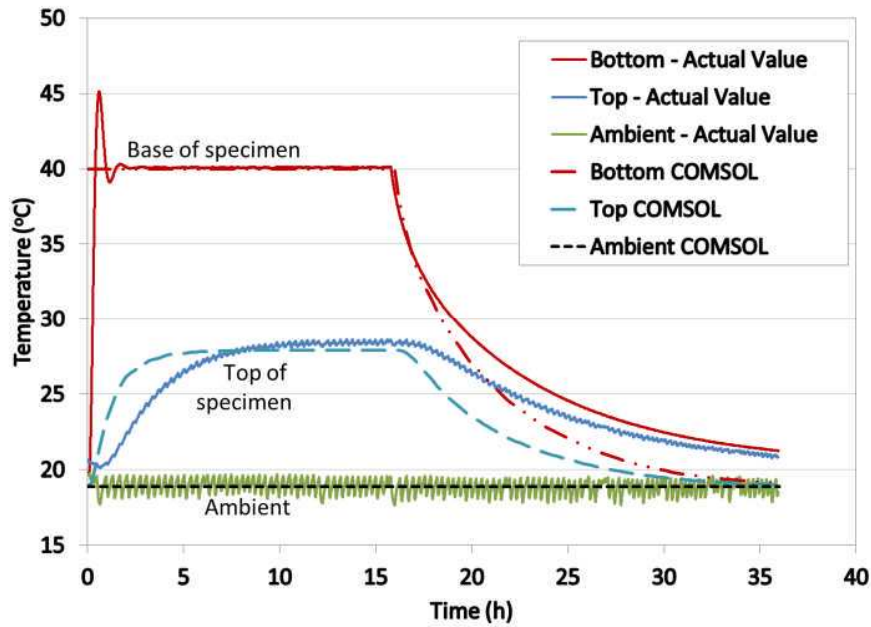
Figure 10 Comparison of the laboratory and modelled Biot number over time for the UoS thermal cell for the 8.00 – 8.45m depth top specimen. Model assumes a soil thermal conductivity of 1.32 W/mK.
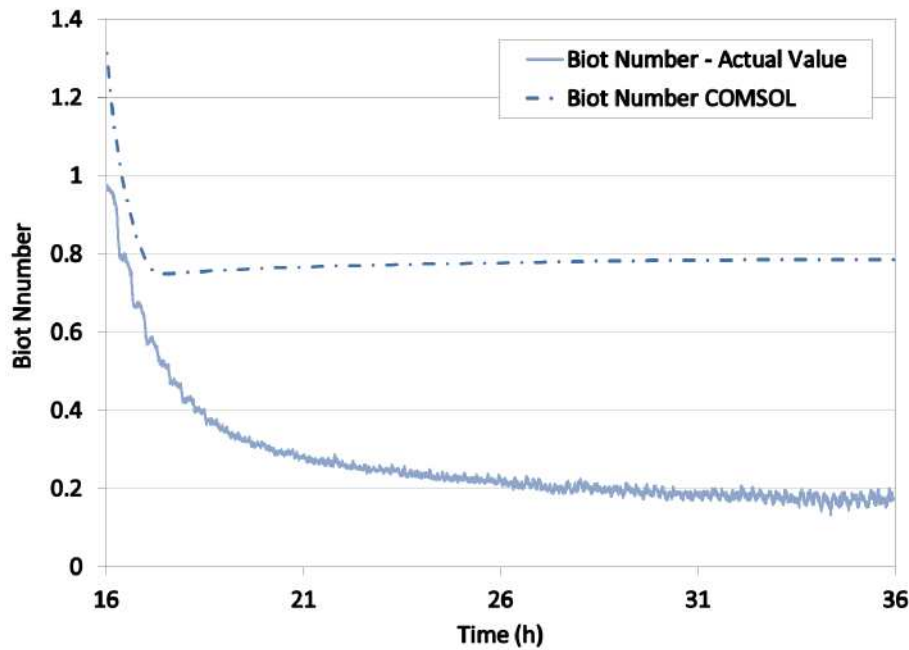
Figure 11 Comparison of the laboratory and modelled temperature variation with time for the Clarke thermal cell for Leighton Buzzard Sand assuming thermal conductivity of 1.4 W/mK and h=4.4 W/m²K.
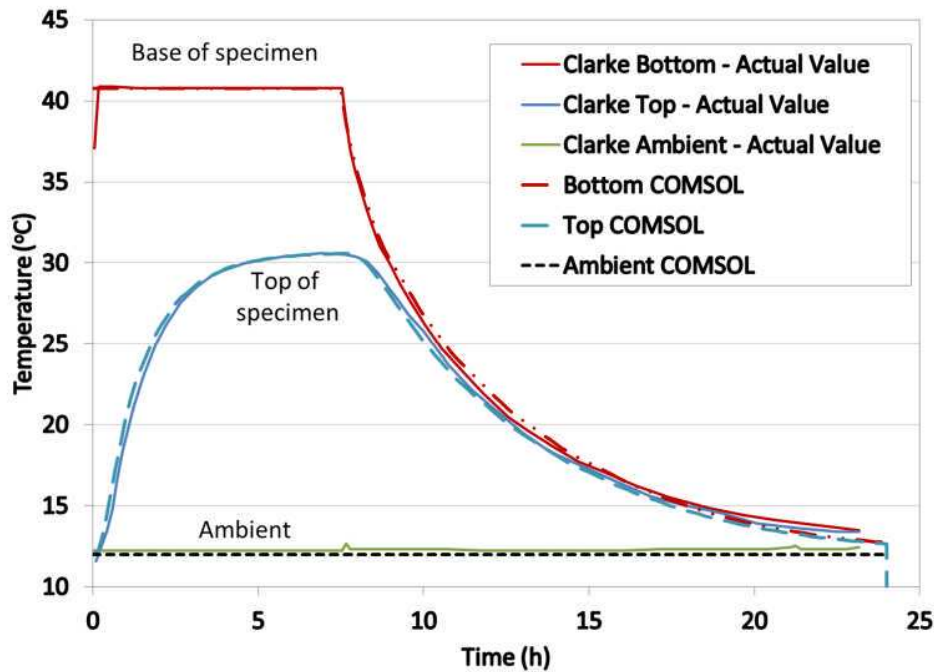

Figure 12 Modelled Biot number for the Clarke thermal cell for Leighton Buzzard Sand assuming a soil thermal conductivity of 1.4 W/mK and a top of specimen heat transfer coefficient of 4.4 W/m²K.
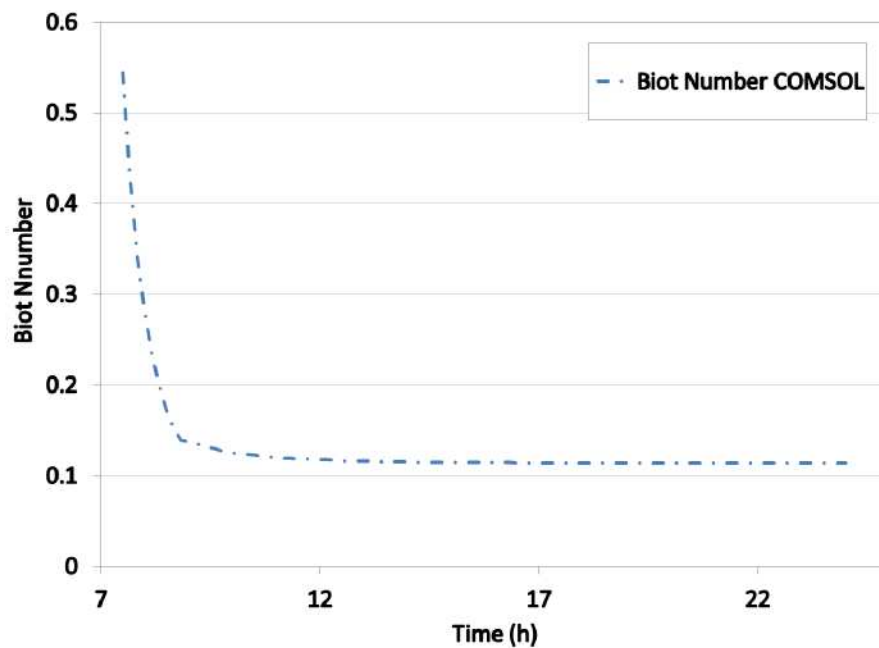
Figure 13 Recovery curves generated by the model idealised thermal cell compared with the theoretical fit curve for different values of soil thermal conductivity.
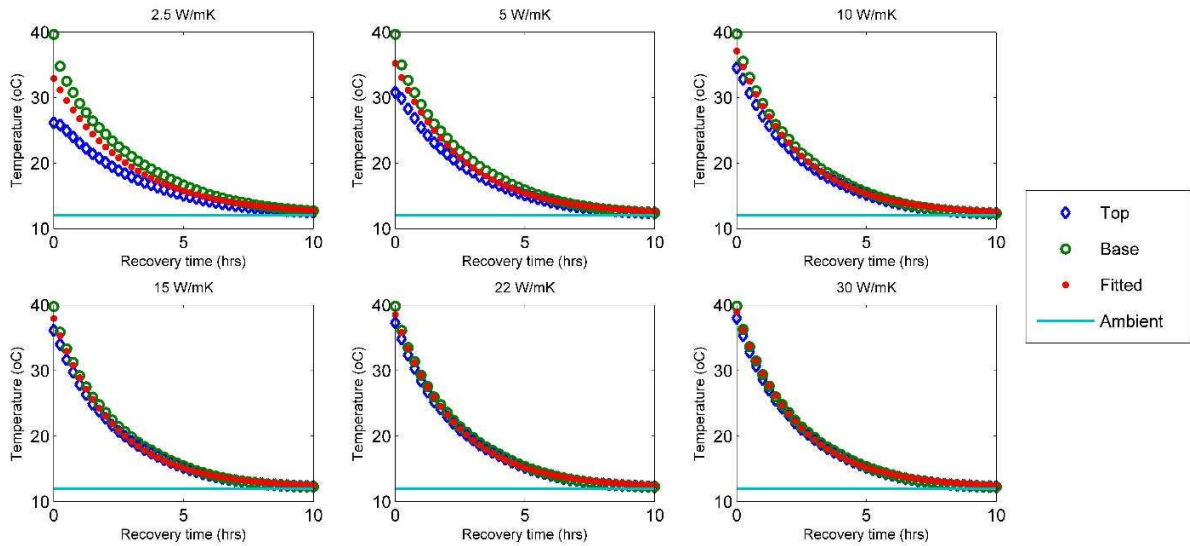

Figure 14 Error in calculated thermal conductivity using the lumped capacitance method, expressed as a percentage of the specified model thermal conductivity assuming an idealised (perfectly insulated) thermal cell.